Please cite this article in press as: Leyva-Díaz et al., FLRT3 Is a Robo1-Interacting Protein that Determines Netrin-1 Attraction in Developing Axons, Current Biology (2014), http://dx.doi.org/10.1016/j.cub.2014.01.042

Current Biology *24*, 1–15, March 3, 2014 ©2014 Elsevier Ltd All rights reserved http://dx.doi.org/10.1016/j.cub.2014.01.042

Article

FLRT3 Is a Robo1-Interacting Protein that Determines Netrin-1 Attraction in Developing Axons

Eduardo Leyva-Díaz,[1] Daniel del Toro,[2,3] Maria José Menal,[4] Serafi Cambray,[4] Rafael Susín,[1] Marc Tessier-Lavigne,[5] Rüdiger Klein,[2,3,6] Joaquim Egea,[4,6,*] and Guillermina López-Bendito[1,6,*]

[1]Instituto de Neurociencias de Alicante, CSIC and Universidad Miguel Hernández, 03550 Sant Joan d'Alacant, Spain

[2]Department of Molecules - Signals - Development, Max Planck Institute of Neurobiology, 82152 Martinsried, Germany

[3]Munich Cluster for Systems Neurology (SyNergy), 80336 Munich, Germany

[4]Molecular and Developmental Neurobiology Group, IRBLLEIDA, University of Lleida, 25198 Lleida, Spain

[5]Laboratory of Brain Development and Repair, Rockefeller University, New York, NY 10065, USA

Summary

Background: Guidance molecules are normally presented to cells in an overlapping fashion; however, little is known about how their signals are integrated to control the formation of neural circuits. In the thalamocortical system, the topographical sorting of distinct axonal subpopulations relies on the emergent cooperation between Slit1 and Netrin-1 guidance cues presented by intermediate cellular targets. However, the mechanism by which both cues interact to drive distinct axonal responses remains unknown.

Results: Here, we show that the attractive response to the guidance cue Netrin-1 is controlled by Slit/Robo1 signaling and by FLRT3, a novel coreceptor for Robo1. While thalamic axons lacking FLRT3 are insensitive to Netrin-1, thalamic axons containing FLRT3 can modulate their Netrin-1 responsiveness in a context-dependent manner. In the presence of Slit1, both Robo1 and FLRT3 receptors are required to induce Netrin-1 attraction by the upregulation of surface DCC through the activation of protein kinase A. Finally, the absence of FLRT3 produces defects in axon guidance in vivo.

Conclusions: These results highlight a novel mechanism by which interactions between limited numbers of axon guidance cues can multiply the responses in developing axons, as required for proper axonal tract formation in the mammalian brain.

Introduction

Understanding how a fairly limited number of axon guidance cues can set up the pattern of connections that is required to form functional neural networks remains a challenge. One explanation may arise from the fact that several axon guidance cues can produce distinct responses depending on the nature and levels of the guidance receptors at the cell surface [1]. The best-documented example of this is Netrin-1, one of the most prominent and influential axon guidance cues for developing axons in the CNS of both vertebrates and invertebrates [2]. Netrins are bifunctional proteins that attract several classes of axons but repel others, depending on the receptors with which they interact on the cell surface and the internal state of the growth cone. The binding of Netrin-1 to the deleted in colorectal carcinoma (DCC) receptor signals attraction, whereas its binding to Unc5-type receptors triggers repulsion [3]. Mechanisms that regulate the surface levels of DCC and Unc5 receptors to control this response to Netrin-1 have been previously reported. For instance, activation of protein kinase C (PKC) leads to the endocytotic internalization of Unc5 receptors, reducing growth cone collapse and changing the response to Netrin-1 from repulsion to attraction [4, 5]. Conversely, protein kinase A (PKA) mobilizes an intracellular pool of DCC, increasing its abundance at the cell surface and enhancing axon outgrowth [6, 7].

The behavior of axons is also regulated by third-party proteins that modulate the responses to the distinct guidance signals [8, 9]. For instance, the Down syndrome cell adhesion molecule (DSCAM) collaborates with DCC in mediating the turning responses of spinal commissural neurons to Netrin-1 [10]. Moreover, Unc5 receptors were also recently shown to bind in *trans* to FLRT3 [11, 12], a member of the fibronectin leucine-rich repeat transmembrane protein family involved in synapse formation and in the regulation of fibroblast growth factor (FGF) receptor signaling [13, 14]. FLRT3 binding to Unc5B receptors activates Unc5 repulsive signaling [15], although how this interaction influences nervous system development has not yet been studied in vivo.

Finally, the axon's responses can be influenced by crosstalk between distinct receptor-signaling pathways involved in guidance [16]. For instance, Netrin-1 attenuates Slit/Robo1 repulsion in precrossing callosal axons to allow them to cross the midline of the developing brain [17], whereas in postcrossing commissural spinal cord axons, the Slit receptor Robo1 silences Netrin-1 attraction to help axons project away from the floor plate [18, 19]. In the thalamocortical system, one of the most prominent higher-level processing connections in the mammalian brain [20], Slit1 acts permissively, conferring responsiveness to Netrin-1 [21]. Whereas Slit1 enables Netrin-1 attraction in a subset of thalamocortical axons (TCAs), for others Slit1 exerts a repulsive response, contributing to the topographical arrangement of this connectivity. Thus, the Slit1 and Netrin-1 cues can be integrated by the axon in a hierarchical, cell-context-dependent manner, whereby one cue might be dominant and suppress the effect of the other (callosal and commissural axons) or might be permissive (such as in specific subsets of TCAs). However, it remains unclear how separate signals are integrated into coherent instructions for correct axon growth.

Here, we discovered a novel mechanism by which crosstalk between axon guidance cues is integrated in developing axons. We found that FLRT3 is a Robo1-interacting protein that acts as a context-dependent modulator of Netrin-1 attraction in thalamic axons. FLRT3 is necessary to gain competence for Netrin-1 attraction and is sufficient to modify the

[6]These authors contributed equally to this work

*Correspondence: joaquim.egea@cmb.udl.cat (J.E.), g.lbendito@umh.es (G.L.-B.)

Please cite this article in press as: Leyva-Díaz et al., FLRT3 Is a Robo1-Interacting Protein that Determines Netrin-1 Attraction in Developing Axons, Current Biology (2014), http://dx.doi.org/10.1016/j.cub.2014.01.042

response to Netrin-1 in Robo1-expressing axons. The mechanism described here might explain how molecularly similar developing axons tune their response to Slit1 and Netrin-1 by simply regulating FLRT3 expression.

Results

Modulation of Netrin-1 Responsiveness Requires DCC Upregulation

We previously showed that developing TCAs are not attracted by Netrin-1 unless the repulsive axon guidance cue Slit1 is present. Moreover, this effect is specific to rostral TCAs (rTCAs) because DCC-expressing intermediate TCAs (iTCAs) are not attracted to Netrin-1, neither alone nor in the presence of Slit1 [21]. Given that rTCAs express DCC under basal conditions but do not respond to Netrin-1, we tested whether the modulation of the Netrin-1 attractive response requires an upregulation of DCC at the membrane in rostral axons. Indeed, the combination of Slit1 and Netrin-1—but neither alone—induced a significant increase in DCC in the membrane of growth cones (Figures 1A–1D′) specifically in rTCAs (Figure 1E). This effect may result from increased vesicular transport to the plasma membrane, because we found a decrease in the pool of internal DCC colocalizing with VAMP2 and Rab11 immunoreactivity [22] upon Slit1 plus Netrin-1 stimulation as compared to the unstimulated basal state (Figures S1A–S1G available online; data not shown), whereas there was an increase in surface DCC (Figures S1A and S1D). These results were confirmed in biotinylation assays (Figures 1F and 1G), raising the possibility that upregulation of DCC might be required to gain competence to respond to Netrin-1 attraction. Indeed, we found that a large proportion of surface DCC colocalizes with Robo1 under basal conditions, whereas this percentage decreased significantly when costimulated with Slit1 and Netrin-1, with an increase in the amount of free DCC receptors at the membrane (Figures S1H–S1O).

It is known that PKA activation is required for the recruitment of DCC-containing vesicles to the plasma membrane [6, 7]. PKA phosphorylates the PP-1 inhibitory protein I-1 (phospho-I-1) in growth cones [23, 24], and thus phospho-I-1 staining is an indicator of PKA activity. We found that phospho-I-1 staining in rTCA growth cones was significantly higher when stimulated with the combination of Slit1 plus Netrin-1 than in control conditions (Figures 1H–1J); this increase was not observed in the presence of a PKA inhibitor (KT5720) or in iTCA growth cones (Figure 1J). Moreover, both an adenylate cyclase inhibitor (SQ22536) and KT5720 abolished the upregulation of DCC at the surface of rTCA growth cones (Figures S1P–S1S), suggesting that the modulation of Netrin-1 responsiveness by Slit1 requires the activation of PKA signaling. The increase in PKA activity in rTCAs was confirmed by western blot (Figures 1K and 1L).

To confirm that DCC is required in rTCAs for the Slit1-induced attractive response to Netrin-1, we confronted rTCA explants (embryonic day 13.5 [E13.5]) from either *Dcc*$^{+/+}$ or *Dcc*$^{-/-}$ mice with aggregates of COS7 cells expressing Netrin-1 in which soluble Slit1 was applied to trigger attraction (Figure 1M). In *Dcc*$^{-/-}$ explants, the Slit1-induced attraction to Netrin-1 was abolished (Figures 1N and 1O) as compared to *Dcc*$^{+/+}$, confirming that DCC function is critical in producing this response. Similar results were found when a well-characterized anti-DCC blocking antibody [25] was used (data not shown).

Slit1 Enables Netrin-1 Attraction through Robo1 Receptor Activation

The fact that Slit1 enables Netrin-1 to attract rTCAs suggests that Robo receptors might be implicated in mediating this behavior. To test this possibility, we examined the response of rTCAs to Netrin-1 plus Slit1 in explants of mice lacking Robo1, Robo2, or both receptors. The attraction to Netrin-1 induced by Slit1 was lost in rTCAs lacking both Robo1 and Robo2 receptors (Figures 2A–2D), demonstrating that activation of Robo receptors is necessary for these TCAs to be attracted to Netrin-1. To determine which of the two Robo receptors was implicated in this process, we confronted rostral thalamic explants from *Robo1* or *Robo2* single mutants with Netrin-1-expressing COS7 cells in the presence or absence of Slit1. When *Robo2*-deficient rTCAs were confronted with Netrin-1 plus Slit1, the attractive response persisted (Figures 2E and 2F). Moreover, Slit1 repulsive activity was lost in *Robo2*$^{-/-}$ rTCAs, but not when explants from *Robo1*-deficient mice were tested (Figure S2), suggesting that Robo1 might modulate the Netrin-1 response rather than mediate the Slit1 repulsive response in these neurons. By contrast, the attractive response to Netrin-1 induced by Slit1 was lost in *Robo1*$^{-/-}$ rTCAs (Figures 2G and 2H), demonstrating the need for Robo1 in the attractive response to Netrin-1.

We assessed whether Robo1 activity might be necessary for the upregulation of cell-surface DCC in rTCAs following exposure to Slit1 and Netrin-1. Unlike in the wild-type controls, surface DCC expression was not upregulated in *Robo1*$^{-/-}$ rTCA growth cones (Figures 2I–2M), demonstrating that Robo1 signaling is necessary to mediate the increase in surface DCC. Consequently, we found that phospho-I-1 levels were not increased in *Robo1*$^{-/-}$ rTCAs by costimulation (Figures 2N–2P), demonstrating the implication of Robo1 receptor in inducing PKA activation by Slit1 and Netrin-1 combination.

Rostral TCAs Express High Levels of FLRT3

Although the results obtained directly implicate the activation of Robo1 in the modulation of Netrin-1 attraction, they do not explain the cell-type specificity, given that iTCAs express similar levels of Robo1 as rTCAs ([21]; Figure S3). Therefore, it seemed necessary to search for other molecular differences that might underlie this specificity. The fibronectin and leucine-rich transmembrane proteins (FLRT1–3) have recently been shown to bind in *trans* to Unc5 receptors [11, 12] and to modulate pyramidal neuron migration within the developing cortex [15]. Thus, we wondered whether, together with Robo1, FLRT proteins might modulate the Netrin-1 response in developing TCAs.

Among the three known FLRT family members, developing thalamic neurons express *Flrt3* mRNA in a decreasing rostral-to-caudal gradient, as witnessed by in situ hybridization (Figures 3A and 3B; data not shown). This gradient was confirmed by X-Gal staining in sections of a FLRT3 reporter line in which β-galactosidase expression is driven by the *Flrt3* promoter (*Flrt3*$^{\beta gal/loxP}$; Figures 3C and 3D) and in dissociated thalamic neurons from these mice, in which the number of neurons expressing β-galactosidase was significantly higher in rostral cultures than in intermediate cultures (Figures 3E–3G). The greater amount of FLRT3 protein in lysates from rostral thalamic cultures corroborated these results (Figures 3H and 3I), as was also evident in the growth cones of rostral thalamic neurons (Figures 3J–3M′). Together, these results show that FLRT3 is specifically enriched in rTCAs, and, therefore, it may play a role in the development of their axons.

Please cite this article in press as: Leyva-Díaz et al., FLRT3 Is a Robo1-Interacting Protein that Determines Netrin-1 Attraction in Developing Axons, Current Biology (2014), http://dx.doi.org/10.1016/j.cub.2014.01.042

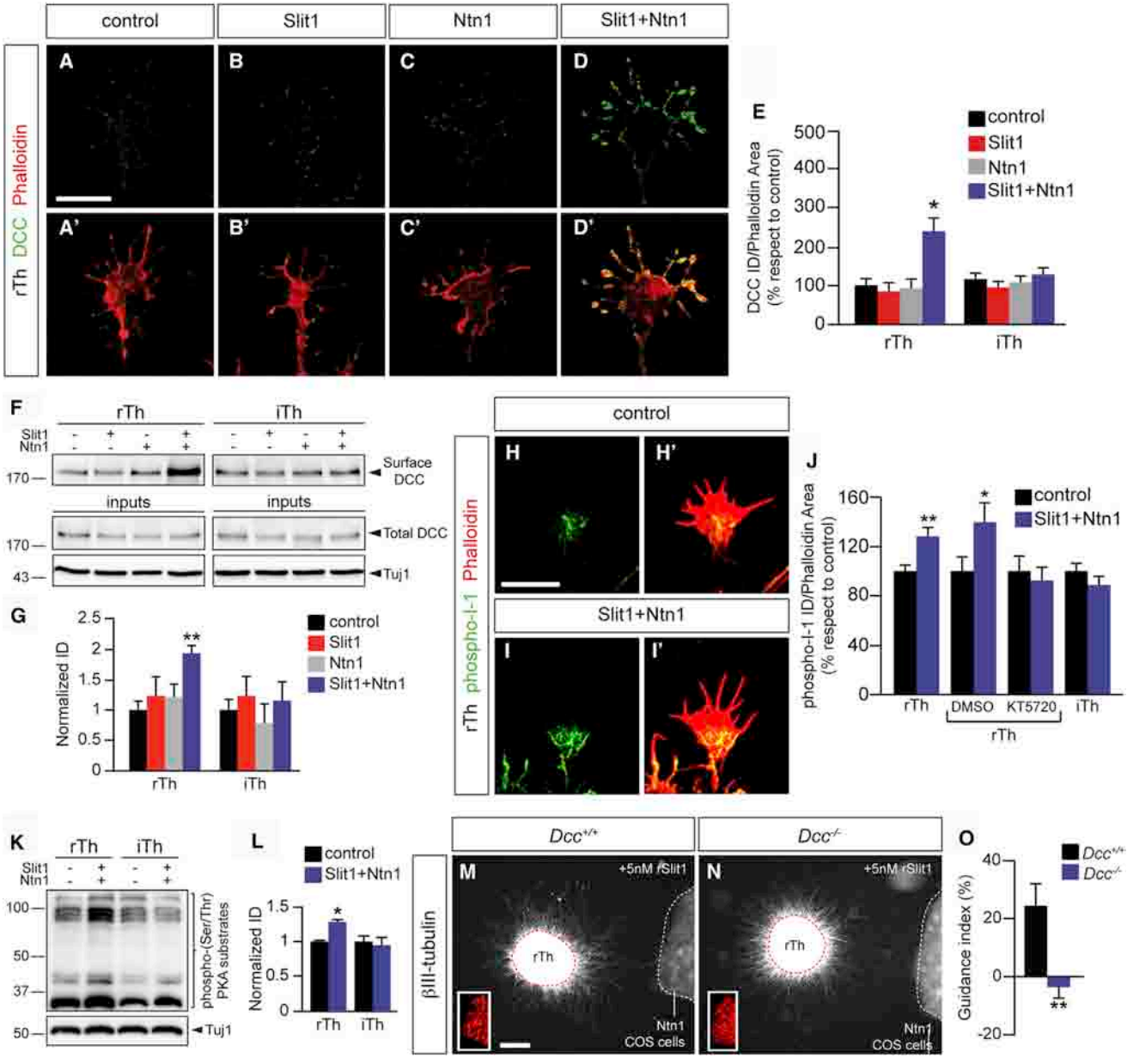

Figure 1. Modulation of Netrin-1 Responsiveness Requires DCC Upregulation

(A–D′) Quantitative DCC surface immunostaining analyzed in nonpermeabilized E13.5 rostral cultured thalamic neurons after 2 days in vitro, both in control conditions and when stimulated with rSlit1 (0.25 μg/ml) plus rNetrin-1 (0.5 μg/ml) for 20 min.

(E) Quantification of the data shown in (A)–(D) and from intermediate thalamic neurons. n ≥ 80 growth cones per condition. *p < 0.05, one-way ANOVA test with Tukey's post hoc analysis.

(F) Surface biotinylation of E13.5 thalamic cultures unstimulated or stimulated with rSlit1 (0.25 μg/ml), rNetrin-1 (0.5 μg/ml), or rSlit1 plus rNetrin-1 for 20 min.

(G) Quantification of the data shown in (F). n = 5. **p < 0.01, two-tailed Student's t test.

(H–I′) Phospho-I-1 staining of E13.5 rostral thalamic neurons cultured for 48 hr, both in control conditions or when stimulated with rSlit1 (0.25 μg/ml) plus rNetrin-1 (0.5 μg/ml) for 20 min.

(J) Quantification of the data represented in (H) and (I) and data not shown. Rostral thalamic growth cones were also treated for 15 min with DMSO or 200 nM KT5720 prior to the addition of the rSlit1 plus rNetrin-1 combination. n ≥ 61 growth cones per condition. *p < 0.05, **p < 0.01, two-tailed Student's t test.

(K) Western blot probed with an anti-phosphorylated PKA substrate antibody recognizing a conserved PKA phosphorylation motif. E13.5 rostral and intermediate thalamic neurons were cultured for 48 hr and unstimulated or stimulated with rSlit1 (0.25 μg/ml) plus rNetrin-1 (0.5 μg/ml) for 20 min.

(L) Quantification of the data shown in (K). n = 2. *p < 0.05, two-tailed Student's t test.

(M and N) Wild-type rTCAs were attracted to Netrin-1-expressing COS7 cells in the presence of rSlit1 (M), whereas $Dcc^{-/-}$ rTCAs grew symmetrically (N). Insets in the lower left corner show dsRed expression in the COS7 cell aggregates.

(O) Quantification of the data represented in (M) and (N). n = 15 $Dcc^{+/+}$ explants; n = 28 $Dcc^{-/-}$ explants. **p < 0.01, two-tailed Student's t test.

rTh, rostral thalamus; iTh, intermediate thalamus; ID, integrated density; rSlit1, recombinant Slit1 protein. The data are presented as the mean + SEM. Scale bars represent 10 μm (A–D′), 5 μm (H–I′), and 150 μm (M and N). See also Figure S1.

Please cite this article in press as: Leyva-Díaz et al., FLRT3 Is a Robo1-Interacting Protein that Determines Netrin-1 Attraction in Developing Axons, Current Biology (2014), http://dx.doi.org/10.1016/j.cub.2014.01.042

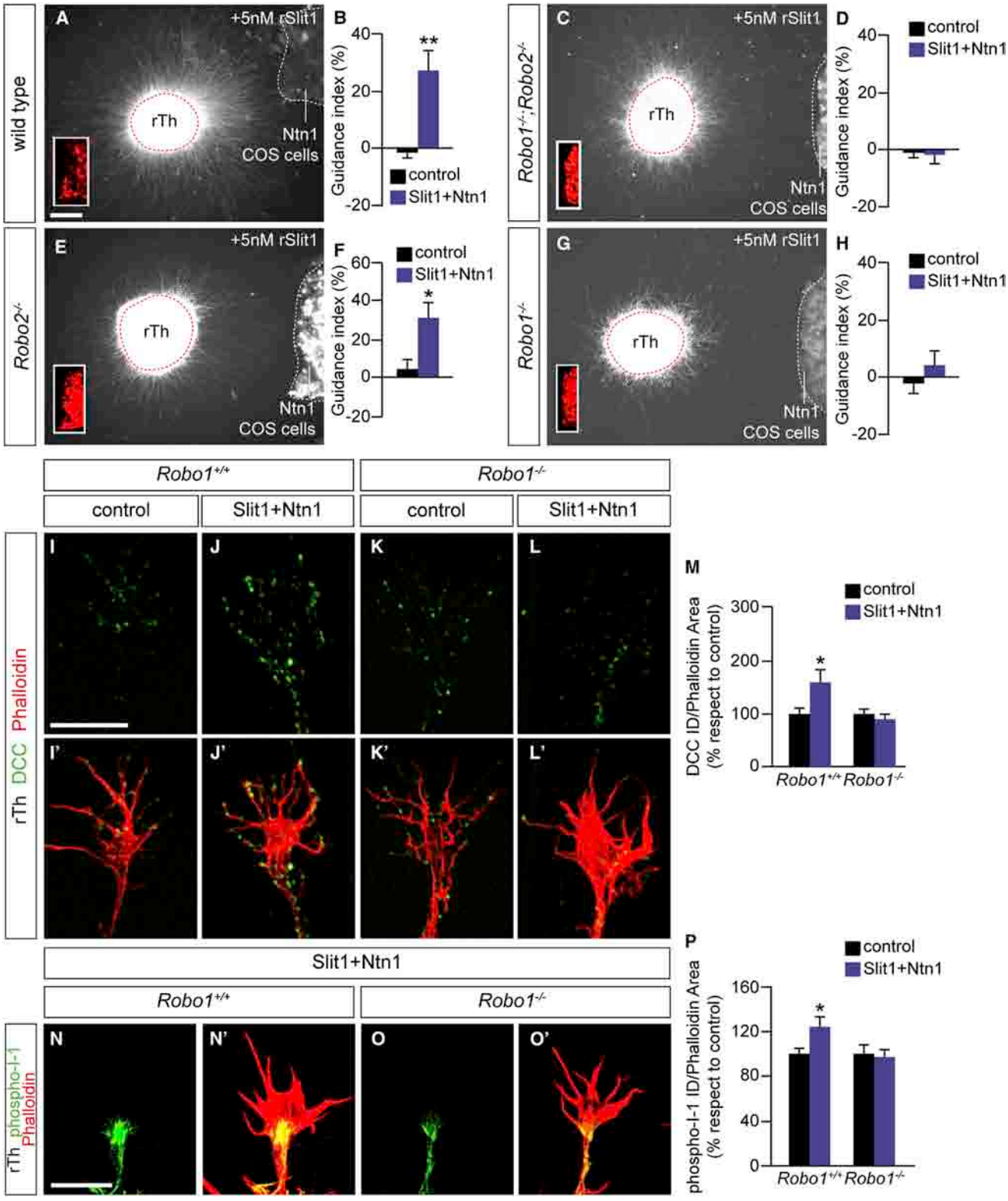

Figure 2. Slit1 Enables Netrin-1 Attraction by Activating the Robo1 Receptor

(A–H) Wild-type (A) and *Robo2*$^{-/-}$ (E) rTCA explants are attracted to Netrin-1-expressing COS7 cells in the presence of rSlit1, while explants lacking the Robo1 receptor (C, *Robo1*$^{-/-}$;*Robo2*$^{-/-}$ and G, *Robo1*$^{-/-}$) grow symmetrically. n $\geq$ 32 wild-type explants per condition; n $\geq$ 32 *Robo1*$^{-/-}$;*Robo2*$^{-/-}$ explants per condition; n $\geq$ 9 *Robo2*$^{-/-}$ explants per condition; n $\geq$ 27 *Robo1*$^{-/-}$ explants per condition. *p < 0.05, **p < 0.01, two-tailed Student's t test.

(I–L′) DCC surface immunostaining of nonpermeabilized *Robo1*$^{+/+}$ (I–J′) and *Robo1*$^{-/-}$ (K–L′) growth cones from E13.5 rostral cultured thalamic neurons after 2 days in vitro.

(legend continued on next page)

Please cite this article in press as: Leyva-Díaz et al., FLRT3 Is a Robo1-Interacting Protein that Determines Netrin-1 Attraction in Developing Axons, Current Biology (2014), http://dx.doi.org/10.1016/j.cub.2014.01.042

FLRT3 Is a New Robo1-Interacting Protein

To better understand the possible function of FLRT3 in the thalamus, we used the mouse FLRT3 intracellular domain ($FLRT3^{ICD}$, amino acids 553–649) as bait in a yeast two-hybrid screen of a human fetal brain cDNA library (Figure S4A). Among the positive hits, one cDNA encoded the Robo1 protein (amino acids 449–1,182; Figures S4B and S4C), while Robo2 was not detected as an interacting partner. Robo1 and FLRT3 interaction was validated in coimmunoprecipitation experiments performed on HEK293T cells transiently transfected with full-length Robo1 and FLRT3 cDNAs (Figures 4A–4D). Deletion of the intracellular domain (ICD) of FLRT3 (Figure 4A) or that of Robo1 (Figure 4E) abolished this association, suggesting that the interaction between Robo1 and FLRT3 takes place mainly in *cis* through their cytoplasmic domains.

Robo1 ICDs are known to be required for Slit1-mediated repulsion [26, 27], and therefore, the binding of FLRT3 to the cytoplasmic domains of Robo1 could modify its repulsive activity. To test this, we performed growth cone collapse assays in response to Slit1, comparing FLRT3-positive rTCAs with FLRT3-negative iTCA neurons. We used $Robo2^{-/-}$ cultures to avoid Robo2 receptor interference in the assay. Both $Robo2^{+/+}$ and $Robo2^{-/-}$ iTCA growth cones collapse in response to Slit1 (Figure S4H), suggesting that Robo1 function is enough to mediate Slit1 repulsive activity in these axons. However, while Slit1 collapsed $Robo2^{+/+}$ rTCA growth cones, Slit1 repulsive activity was abolished in $Robo2^{-/-}$ rTCA growth cones (Figures S4D–S4H). Together with the lack of Slit1-mediated repulsion in rTCA from *Robo2* mutants that we have previously observed (Figures S2G–S2I), these data suggest that FLRT3 present in rTCAs may modulate Slit1/Robo1 repulsion.

Finally, we detected Robo1 when FLRT3 was immunoprecipitated from protein extracts of dissociated thalamic neurons (Figure 4F), and these two proteins colocalized in rostral thalamic growth cones (Figures 4G–4K), strongly suggesting that they interact in TCAs.

FLRT3 Is Necessary to Mediate Slit1-Induced Netrin-1 Attraction

Because Robo1 is required by rTCAs for the Slit1-induced switch in Netrin-1 responsiveness, we tested whether FLRT3 activity is also involved in this process. As such, we confronted control and *Flrt3* nervous system conditional mutant ($Flrt3^{\beta gal/lx;NesCre}$) rostral thalamic explants with COS7 cells expressing Netrin-1 in the presence of Slit1. The lack of FLRT3 abolished the switch toward Netrin-1 attraction (Figures 5A–5C), demonstrating that FLRT3 and Robo1 are both necessary for such attraction to occur. The addition of a recombinant protein containing only the extracellular domain of FLRT3 to these cultures did not elicit attraction to the Netrin-1 stimuli of the *Flrt3*-conditional mutant rTCAs (Figure S5), suggesting that the intracellular domain of the FLRT3 protein is crucial for attraction to occur. Moreover, the fact that FLRT3 interacts with Robo1 in thalamic neurons (Figure 4F) and that a large percentage of the surface FLRT3 colocalizes with Robo1 in rostral growth cones (Figures 4G–4K) suggest that the function of FLRT3 in mediating this attraction might be due to its interaction with the Robo1 signaling pathway.

Having shown that DCC upregulation at the membrane strongly correlated with the switch toward Netrin-1 attraction, we tested whether this upregulation occurred in the absence of *Flrt3*. Unlike control TCAs, the combination of Slit1 and Netrin-1 did not induce an increase in surface DCC levels in *Flrt3* conditional mutant rTCAs (Figures 5D–5H). Furthermore, the increase in phospho-I-1 induced by Slit1 and Netrin-1 costimulation did not occur in rTCAs in the absence of *Flrt3* (Figures 5I–5K). Altogether, these results strongly suggest that FLRT3 and Robo1 modulate the Netrin-1 response in developing rTCAs by increasing the abundance of DCC receptors at the plasma membrane of the growth cones via PKA activation.

FLRT3 Expression Is Sufficient to Alter the Response to Netrin-1 in Robo1-Expressing Axons

Robo1 and FLRT3 levels remain unchanged in rostral thalamic growth cones of *Flrt3* conditional mutant and in $Robo1^{-/-}$ mutant mice, respectively (Figure S6). Hence, it would appear that neither Robo1 nor FLRT3 activity alone is sufficient to trigger the attractive behavior and that both proteins must be present. Thus, we hypothesized that ectopic expression of FLRT3 in nonresponsive iTCAs that contain Robo1 may be sufficient to trigger this attractive behavior. Indeed, electroporation of a *Flrt3* expression vector into iTCAs specifically provoked the switch toward Netrin-1 attraction (Figures 6A–6D), demonstrating that FLRT3 expression is sufficient to modulate the Netrin-1 response in axons that express Robo1. We further asked whether FLRT3 overexpression in nonresponsive iTCAs would be sufficient to drive their axons to a more rostral position in the ventral telencephalon, in a manner similar to rostral axons. To test this, we determined the function of FLRT3 in iTCA pathfinding ex vivo by coculturing intermediate explants expressing *Flrt3* in 45° corridor host slices [21] (Figure 6E). Whereas mock-electroporated intermediate axons navigated at rostro-intermediate levels in the subpallium, most of the axons expressing *Flrt3* grew rostrally (Figures 6F–6H), again indicating that FLRT3 is sufficient to transform the behavior of iTCAs to that of rTCAs. Moreover, because we hypothesized that the ability of FLRT3 to change iTCA behavior depends on the presence of Robo1, we performed similar coculture experiments using iTCA explants from $Robo1^{+/+}$ or $Robo1^{-/-}$ embryos electroporated with *Flrt3* and cocultured into wild-type 45° corridor host slices (Figure 6I). Ectopic expression of FLRT3 in intermediate thalamic neurons mutant for *Robo1* was not able to transform the behavior of iTCAs (Figures 6J–6L), demonstrating that both receptors are necessary to trigger the attractive response.

Finally, phospho-I-1 staining after Slit1 and Netrin-1 costimulation was significantly higher in iTCA growth cones by the ectopic expression of FLRT3 (Figures 6M–6P), strongly suggesting the involvement of PKA activity in the mechanism of switch in Netrin-1 responsiveness.

Abnormal Pathfinding of TCAs in the Absence of FLRT3 In Vivo

Specifically, a decreasing rostral-to-caudal gradient of Slit1 and Netrin-1 is provided by corridor cells in the ventral

(M) Quantification of the data shown in (I)–(L). n ≥ 80 growth cones per condition. *p < 0.05, two-tailed Student's t test.
(N–O′) Phospho-I-1 staining on $Robo1^{+/+}$ (N) or $Robo1^{-/-}$ (O) E13.5 rostral thalamic growth cones.
(P) Quantification of the data represented in (N) and (O) and data not shown. n ≥ 89 growth cones per condition. *p < 0.05, two-tailed Student's t test.
rTh, rostral thalamus; rSlit1, recombinant Slit1 protein; ID, integrated density. The data are presented as the mean + SEM. Scale bars represent 150 μm (A–G), 10 μm (I–L′), and 5 μm (N–O′). See also Figure S2.

Please cite this article in press as: Leyva-Díaz et al., FLRT3 Is a Robo1-Interacting Protein that Determines Netrin-1 Attraction in Developing Axons, Current Biology (2014), http://dx.doi.org/10.1016/j.cub.2014.01.042

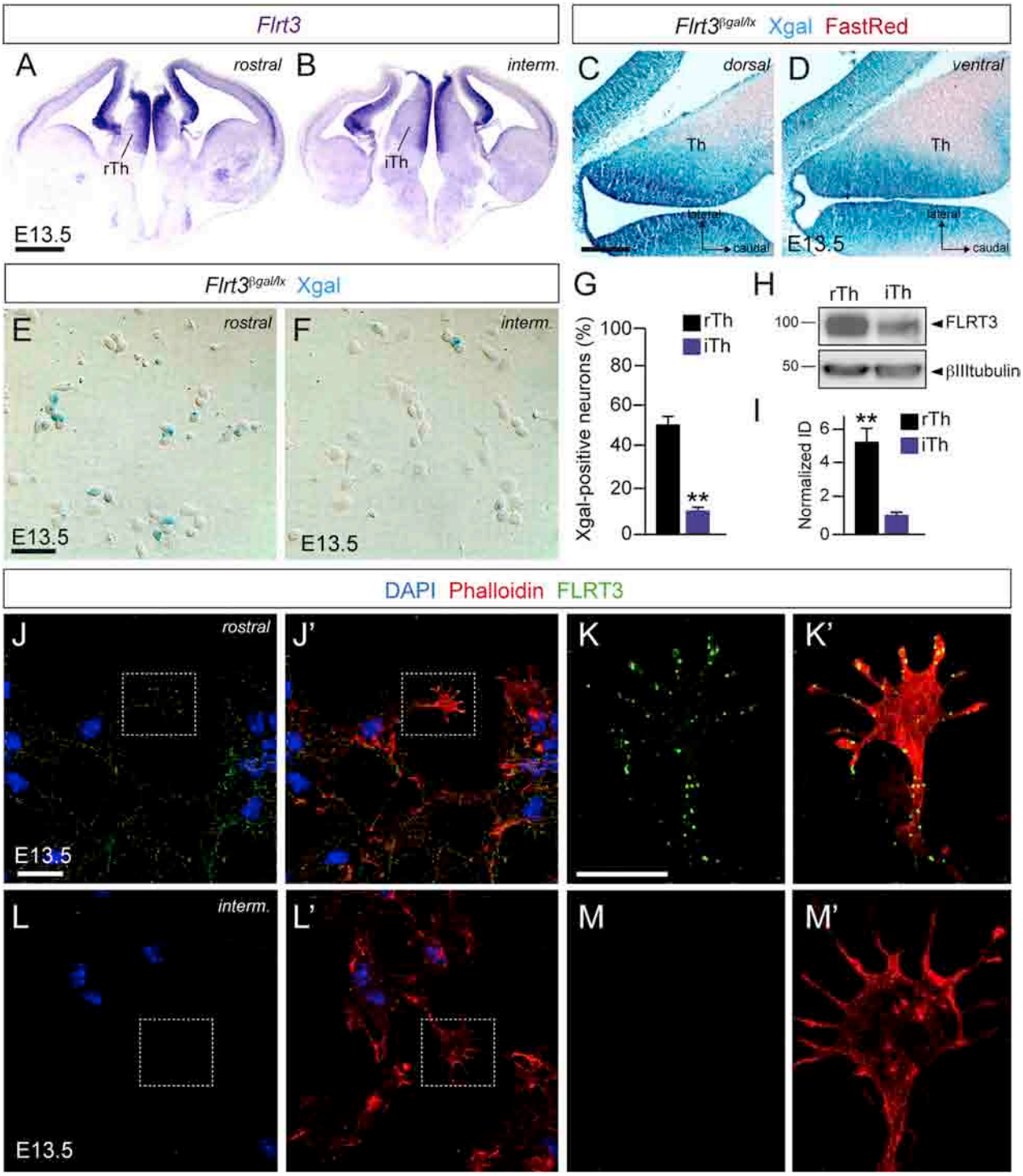

Figure 3. Rostral TCAs Express High Levels of FLRT3

(A and B) Serial coronal sections through the telencephalon of E13.5 embryos showing *Flrt3* expression by in situ hybridization.

(C and D) Serial horizontal sections through the telencephalon of E13.5 embryos from a *Flrt3*$^{\beta gal/lx}$ reporter line counterstained with FastRed.

(E and F) X-Gal staining of dissociated thalamic *Flrt3*$^{\beta gal/lx}$ cultures showing fewer β-gal stained neurons among the intermediate thalamic neurons than in the rostral neurons.

(G) Quantification of the data presented in (E) and (F). n = 1,933 rTh cells, n = 1,246 iTh cells. **p < 0.01, two-tailed Student's t test.

(H) Western blot showing FLRT3 protein levels in lysates from E13.5 rostral or intermediate thalamic neurons cultured for 48 hr.

(I) Quantification of the data shown in (H) (n = 3). **p < 0.01, two-tailed Student's t test.

(J–M′) FLRT3 surface staining of nonpermeabilized rostral (J–K′) and intermediate (L–M′) dissociated thalamic cultures showing stronger expression in rostral axons.

rTh, rostral thalamus; iTh, intermediate thalamus; interm., intermediate. The data are presented as mean + SEM. Scale bars represent 1 mm (A and B), 200 μm (C and D), 30 μm (E and F), 20 μm (J, J′, L, L′), and 10 μm (K, K′, M, M′). See also Figure S3.

Please cite this article in press as: Leyva-Díaz et al., FLRT3 Is a Robo1-Interacting Protein that Determines Netrin-1 Attraction in Developing Axons, Current Biology (2014), http://dx.doi.org/10.1016/j.cub.2014.01.042

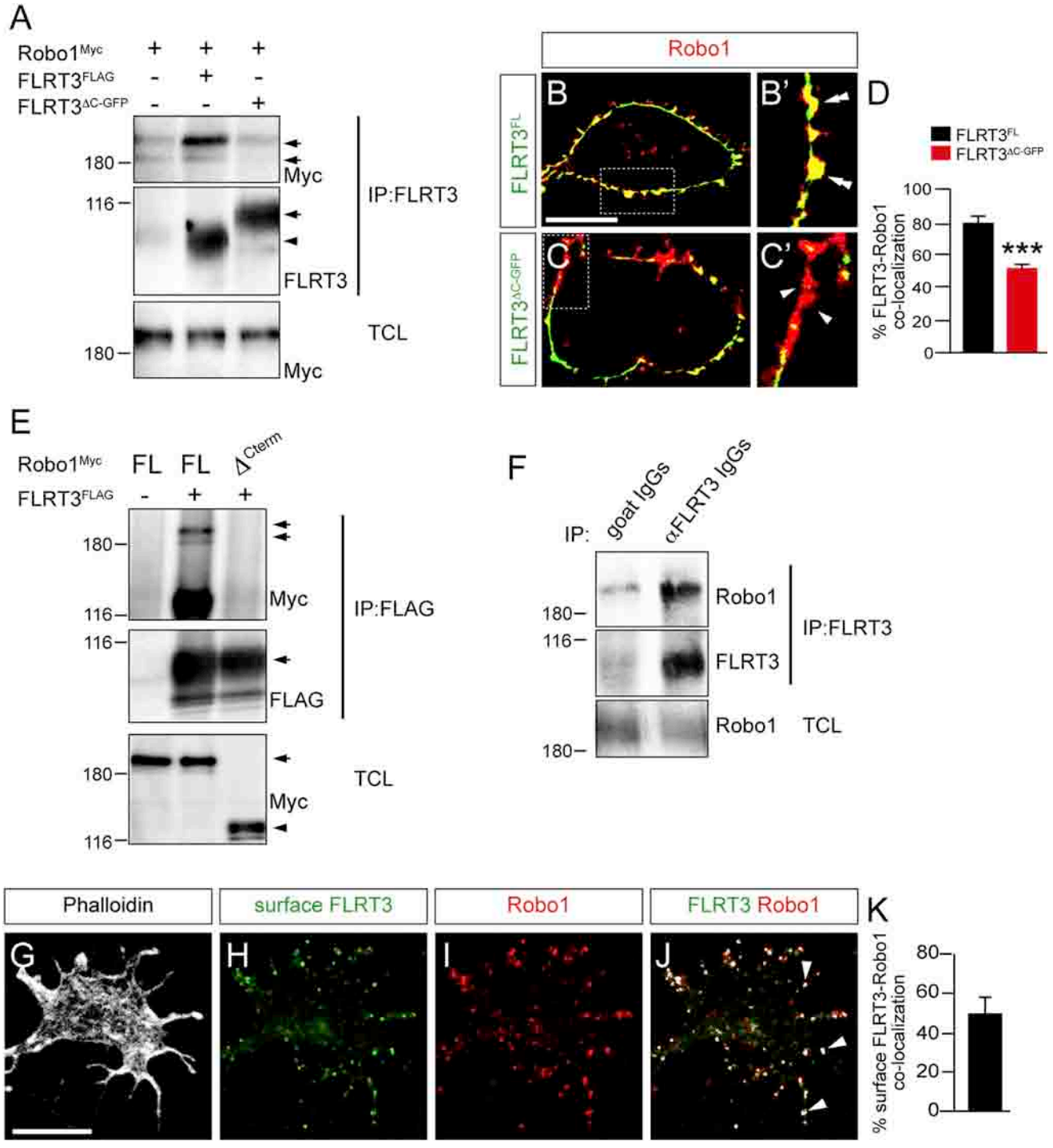

Figure 4. FLRT3 Is a New Robo1-Interacting Protein

(A) FLRT3-Robo1 coimmunoprecipitation in HEK293T cells. As indicated, myc-tagged Robo1, FLRT3, and FLRT3ΔC-GFP were transiently transfected into HEK293T cells. The protein lysates were immunoprecipitated with an anti-FLRT3 antibody, and the immunoprecipitates were analyzed in western blots probed with antibodies against Myc (upper panel) and FLRT3 (middle panel). The lower panel shows the Robo1 in the total cell lysates (TCL). In the middle panel, the arrow indicates FLRT3ΔC-GFP, and the arrowhead indicates full-length FLRT3.

(B and C) Colocalization of Robo1 and FLRT3 in HEK293T cells. The cells were cotransfected with full-length FLRT3 ($FLRT3^{FL}$; B) or FLRT3ΔC-GFP (C) and Robo1 and then fixed and analyzed by immunofluorescence.

(D) The percentage of Robo1 clusters at the membrane where FLRT3 was also detected (asterisks in B′) was quantified and referred to total Robo1 clusters. Arrowheads in (C′) point to clusters without FLRT3. n > 10 cells. ***p < 0.001, two-tailed Student's t test.

(E) Myc-tagged Robo1 lacking the entire ICD (ΔC Robo1) was cotransfected into HEK293T cells with FLRT3 as indicated (full-length [FL] Robo1 was used as a control). Anti-FLAG immunoprecipitates were analyzed in western blots probed with antibodies against Myc (upper panel) and FLAG (middle panel). The lower panel shows the Robo1 in the TCL. The arrows indicate the position of the specific proteins, and the arrowhead in the lower panel shows the position of ΔC Robo1.

(legend continued on next page)

telencephalon (vTel) to attract the rTCAs toward the rostral regions of this structure and ultimately, the cortex [21]. Our data suggest that FLRT3 is sufficient to modulate the response of axons expressing Robo1 to Netrin-1. To test whether FLRT3 is indeed necessary for the positioning of rTCAs in vivo, we performed fine anterograde labeling of the rostral thalamus with DiI in *Flrt3* conditional mutant brains (Figures 7A–7D). We reproducibly observed that in the absence of FLRT3, rTCAs dispersed toward more intermediate levels than in controls, demonstrating that the fine positioning of rTCAs requires FLRT3 activity in these axons. Although the expression patterns for *Slit1* and *Netrin-1* in the vTel are normal in *Flrt3* conditional mutant brains (Figure S7), we performed analysis of the development of rTCAs in a transgenic mouse in which *Flrt3* is specifically removed from the thalamus (*Flrt3*$^{lx/lx;Gbx2CreER}$; Figures 7E–7H). The conditional *Flrt3* removal from the thalamus mimics the phenotype found in the *Flrt3* nervous system conditional knockout, demonstrating that *Flrt3* expressed in rTCAs is necessary for acquiring their correct topographical information.

Both FLRT3 and Robo1 are necessary to guide rTCAs by changing Netrin-1 responsiveness. Thus, we reasoned that the absence of *Robo1*, but not *Robo2*, should mimic the defect found in *Flrt3* conditional mutant brains. Indeed, rTCAs dispersed more toward intermediate levels in *Robo1*$^{-/-}$ mice than in control mice (Figures 7I–7L), while rTCA dispersion was normal in *Robo2*$^{-/-}$ mice (Figure 7L). Together, these results show that both FLRT3 and Robo1 are required to modulate the response of TCAs to Netrin-1.

In summary, our results demonstrate that the positioning of distinct TCAs that express similar levels of axon guidance receptors is achieved by modulating their response to Netrin-1 through the activity of FLRT3.

Discussion

The correct formation of neural circuits depends on the ability of growing axons to resolve and integrate information from multiple sources when navigating through complex cellular environments. Here, we found that FLRT3 acts as a coreceptor of the Robo1 receptor and that it is required in rTCAs to modulate their Netrin-1 responsiveness in a manner that is crucial for their topographic positioning. Slit1 and Netrin-1 lead to the upregulation of DCC at the surface of the growth cone and to the Netrin-1 attraction through the synergistic action of Robo1 and FLRT3 (Figures 7M and 7N). This FLRT3-Robo1 interaction only occurs in rostral axons, because although iTCAs express DCC and Robo1 receptors, they do not contain FLRT3 and, thus, they are not attracted to Netrin-1. Therefore, our study shows that two different guidance cues, such as Slit1 and Netrin-1, cooperate to modify axonal behaviors through enhancing downstream signals (e.g., PKA), which trigger expression changes of a guidance receptor on the cell surface. Broadly, FLRT3 might act as a context-dependent modulator of axon guidance signals, and this function may emerge as a prevalent strategy to ensure the sequential switching in axon guidance responses that is necessary to correctly guide developing axons.

Netrin-1 Attraction Involves PKA Activation and DCC Upregulation by Slit1 and Netrin-1

We have shown that the response to Netrin-1 by rTCAs requires the upregulation of surface DCC through cAMP/PKA activation. These results are consistent with the general idea that increases in local cAMP promote axon attraction [28] and with previous findings in commissural neurons showing that PKA activation translocates DCC to the plasma membrane, thereby promoting axon growth and axon turning in response to Netrin-1 [6, 7, 29]. Intracellular DCC pools are more than likely mobilized from microtubule-associated transport vesicles (VAMP2-positive; Figure S1) that are thought to be involved in asymmetric exocytosis during attraction [30]. Intriguingly, although cAMP can modulate the response of axons to Netrin-1, Netrin-1 stimulation of developing axons does not seem to alter endogenous cAMP levels, and thus, other signals would appear to be necessary to activate PKA [31]. We believe that Slit1 signaling is important in this regard, most likely in a crosstalk with Netrin-1 signaling, because DCC is only upregulated at the plasma membrane of rTCAs upon costimulation with Slit1 plus Netrin-1. Thus, it is possible that Slit1 and Netrin-1 signaling are both synergistically required to reach a certain threshold of PKA activation, explaining the requirement for the combination of cues. Thus, PKA could function as a coincidence detector that integrates two different signals in rTCAs, ensuring that the attractive response will only occur when Slit1 and Netrin-1 are present, similar to the proposed role for Ret in axons from the lateral motor column at the spinal cord [8].

Slit/Robo use Rac-specific GTPase-activating proteins (GAPs) and guanine nucleotide exchange factors (GEFs) as intracellular signaling proteins to mediate repulsion [32]. Although variations in cAMP levels modulate Robo-mediated repulsion [33, 34], a direct link between Robo signaling and cAMP/PKA activation has not been reported to date. Thus, it is tempting to speculate that activation of the FLRT3-Robo1 complex by Slit1 in rTCAs might shift the default Robo intracellular cascade from Rac toward PKA activation. Further experiments to explore this possibility are called for.

The Convergence of Slit1 and Netrin-1 Signaling in Developing Axons

In precrossing callosal axons, Netrin-1 attenuates Slit/Robo1 repulsion in order to allow axons to cross the midline in the developing brain [17], whereas in postcrossing commissural spinal cord axons, the Slit receptor Robo1 silences Netrin-1 attraction to help axons project away from the floor plate [18, 19]. In basal conditions, rostral thalamic axons and callosal axons apparently behave similarly, in the sense that Netrin-1 does not exert any chemotactic effect on its own. However, Netrin-1 has two different functions in these systems: its main role in callosal axons is to attenuate Robo signaling and allow the axons to cross the midline, whereas

(F) FLRT3-Robo1 coimmunoprecipitation in rTCA neurons. Protein extracts of E13.5 rostral cultured thalamic neurons after 2 days in vitro were immunoprecipitated with a control goat IgG or with anti-FLRT3 IgGs (raised in goat). The immunoprecipitates were analyzed in western blots probed with antibodies against Robo1 (upper panel) and FLRT3 (middle panel). The lower panel shows the Robo1 in the TCL.

(G–J) FLRT3 surface staining of nonpermeabilized rostral neurons, followed by Robo1 staining, and with phalloidin staining showing the growth cone morphology in white. Arrowheads in (J) indicate colocalization spots.

(K) Quantification of the data shown in (J) ($n \geq 60$).

The data are presented as mean + SEM. Scale bars represent 10 μm. See also Figure S4.

Please cite this article in press as: Leyva-Díaz et al., FLRT3 Is a Robo1-Interacting Protein that Determines Netrin-1 Attraction in Developing Axons, Current Biology (2014), http://dx.doi.org/10.1016/j.cub.2014.01.042

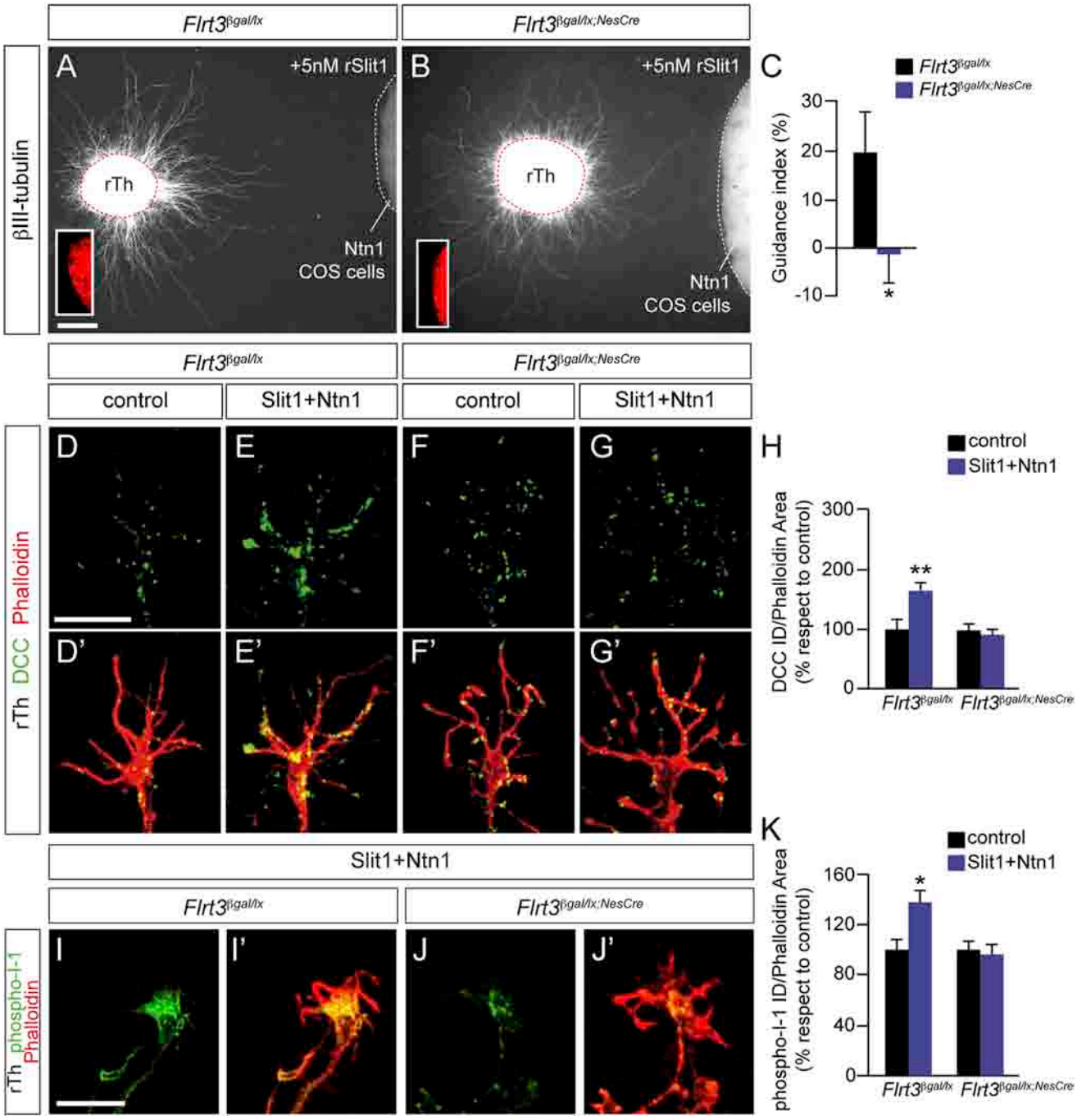

Figure 5. FLRT3 Is Necessary to Mediate Slit1-Induced Netrin-1 Attraction

(A and B) Rostral control (*Flrt3*$^{\beta gal/lx}$) axons are attracted to Netrin-1-expressing COS7 cells in the presence of rSlit1 (A), whereas axons from the conditional *Flrt3*$^{\beta gal/lx;NesCre}$ mutant grow symmetrically (B).

(C) Quantification of the data represented in (A) and (B). n = 25 *Flrt3*$^{\beta gal/lx}$ explants; n = 16 *Flrt3*$^{\beta gal/lx;NesCre}$ explants. *p < 0.05, two-tailed Student's t test.

(D–G′) DCC surface immunostaining of nonpermeabilized *Flrt3*$^{\beta gal/lx}$ (D–E′) and *Flrt3*$^{\beta gal/lx;NesCre}$ (F–G′) E13.5 rostral thalamic neurons.

(H) Quantification of the data represented in (D)–(G). n ≥ 130 growth cones per condition. **p < 0.01, two-tailed Student's t test.

(I–J′) Phospho-I-1 staining on *Flrt3*$^{\beta gal/lx}$ (I) or *Flrt3*$^{\beta gal/lx;NesCre}$ (J) E13.5 rostral thalamic growth cones cultured for 48 hr when stimulated with rSlit1 (0.25 μg/ml) plus rNetrin-1 (0.5 μg/ml) for 20 min.

(K) Quantification of the data represented in (I) and (J) and data not shown. n ≥ 75 growth cones per condition. *p < 0.05, two-tailed Student's t test.

rTh, rostral thalamus; rSlit1, recombinant Slit1 protein; ID, integrated density. The data are presented as mean + SEM. Scale bars represent 150 μm (A and B) and 10 μm (D–G′; I–J′). See also Figure S5.

it becomes chemotactic for rTCAs upon the permissive effect of Slit1. Why Slit1 and Netrin-1 have such different effects on axons crossing the midline and on TCAs is currently unknown. We speculate that on/off decisions that favor hierarchical interactions are taken at the midline. By contrast, topographic maps rely on smooth gradients of signals that trigger more

Please cite this article in press as: Leyva-Díaz et al., FLRT3 Is a Robo1-Interacting Protein that Determines Netrin-1 Attraction in Developing Axons, Current Biology (2014), http://dx.doi.org/10.1016/j.cub.2014.01.042

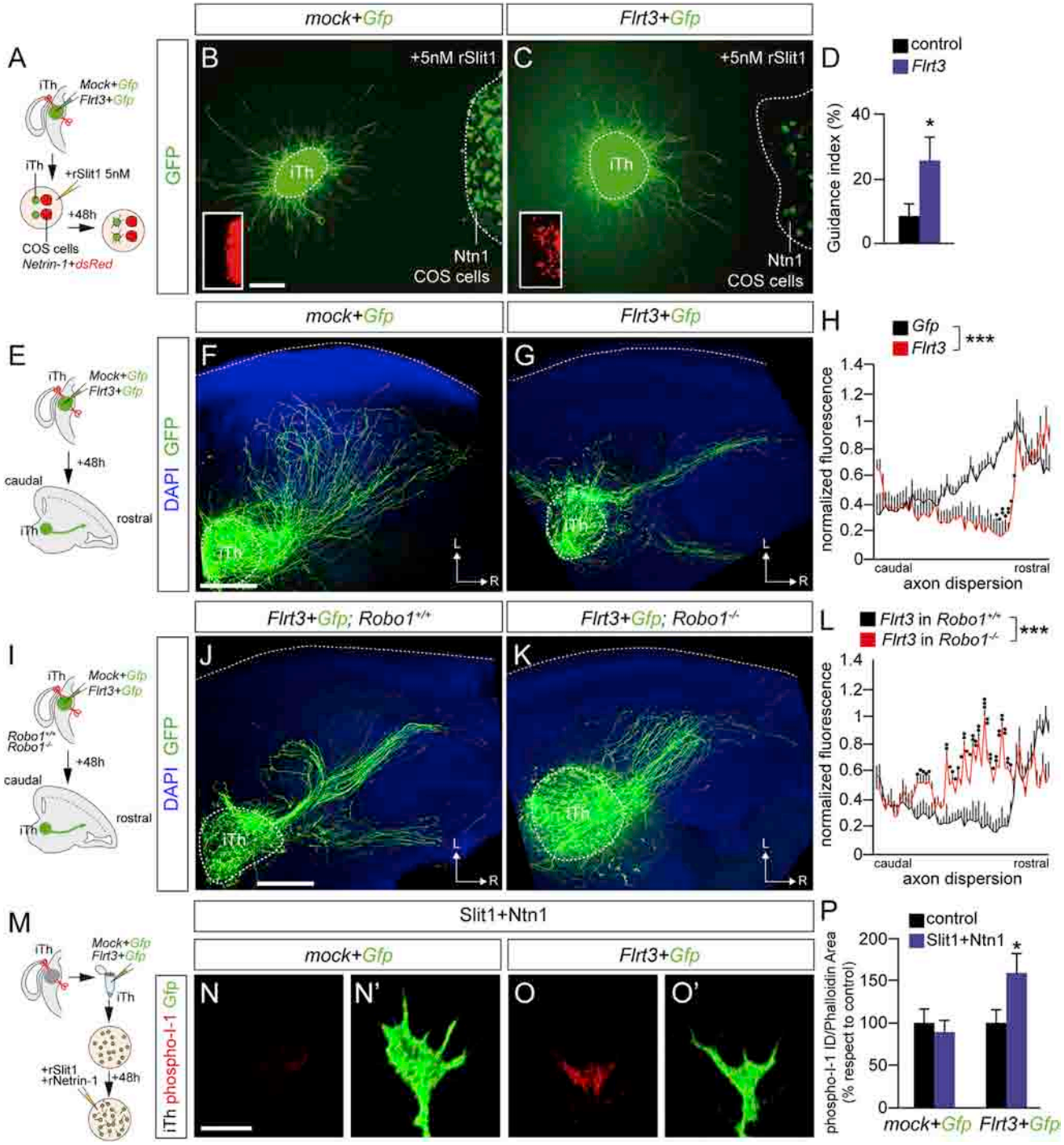

Figure 6. FLRT3 Expression Is Sufficient to Alter the Response to Netrin-1 in Robo1-Expressing Axons

(A) Experimental paradigm used to test the effect of *Flrt3* gain of function.

(B and C) Explants electroporated with control cDNA grow symmetrically when confronted with Netrin-1-expressing COS7 cells in the presence of rSlit1 (B), whereas *Flrt3*-electroporated explants are attracted to this combined stimulus (C).

(D) Quantification of the data represented in (B) and (C). n = 19 explants for mock electroporation; n = 18 explants for full-length *Flrt3* electroporation. *p < 0.05, two-tailed Student's t test.

(E) Experimental paradigm used to test the role of FLRT3 in the navigation of iTCAs.

(F and G) Control-electroporated iTCAs grow at rostro-intermediate positions into the ventral telencephalon of wild-type embryos (F), whereas *Flrt3*-electroporated iTCAs grow rostrally (G).

(H) Quantification of the data represented in (F) and (G). n = 6 mock electroporated cocultures; n = 6 full-length *Flrt3* electroporated cocultures. ***p < 0.001 between distributions; *p < 0.05 and **p < 0.01 between particular points, two-way ANOVA test.

(I) Experimental paradigm used to test the role of FLRT3 in the navigation of iTCAs in the presence or absence of Robo1.

(legend continued on next page)

subtle and complex decisions and that probably involve other types of interactions between guidance cues, such as the permissive effect of Slit1 on Netrin-1 attraction. In this context, such an interaction would be important for the fine topographical sorting of axonal tracts.

Attraction in rTCAs correlates with an increase of DCC at the surface of the growth cone, suggesting that a certain threshold of DCC levels is necessary for the attractive response to Netrin-1. An alternative explanation is that Robo1-DCC interactions silence basal DCC activity, therefore preventing Netrin-1 from being attractive. Accordingly, we have found that Robo1 and DCC interact in thalamic neurons in basal conditions, that DCC-Robo1 immunostaining showed a high colocalization at the surface of rTCA growth cones, and that this colocalization was reduced after Slit1 plus Netrin-1 stimulation. However, when we confronted rTCA explants from either *Robo1* or the double *Robo1;Robo2* knockouts, we did not observe attraction toward Netrin-1, suggesting that DCC silencing is not the major mechanism.

FLRT3 Is a Context-Dependent Modulator of Axonal Responses

Context-dependent permissive interactions between axon-guidance cues, such as the case of NrCAM and GDNF proteins that modulate axon sensitivity to Sema3B in spinal cord axons [35, 36] or the switch of Sema6D activity from repulsive to attractive by NrCAM and plexin-A1 in retinal axons in vitro [37, 38], have already been shown. Therefore, whereas previous reports have suggested that the presence or absence of a coreceptor protein simply induces different downstream signals [39, 40], our study suggests that a coreceptor (FLRT3) changes the surface expression of an additional guidance receptor through promoting downstream signals that in turn convert the responses of axons. FLRT3 might switch Robo1 signaling to enable Netrin-1 attraction by upregulating the levels of DCC in the plasma membrane through PKA activity. Moreover, as we found that FLRT3 interacts in *cis* with the intracellular domain of Robo1 and that Slit1 repulsion is lost in *Robo2* mutants despite the presence of Robo1, our data also suggest that FLRT3 might be a potential modulator of Slit1/Robo1 repulsive responses triggered in rTCAs.

We found no evidence showing that FLRT3 modulates Netrin-1/DCC signaling directly because we did not detect significant binding of Netrin-1 to FLRT3, nor were we able to coimmunoprecipitate FLRT3 and DCC (data not shown). Moreover, we did not find that Slit1 binds directly to FLRT3 or that Slit1 changes the affinity of the Robo1-FLRT3 interaction (data not shown), leading us to consider the possibility that FLRT3 may be activated by an unknown ligand or that FLRT3 acts independently of a direct ligand, at least in this context. In this latter scenario, FLRT3 might simply modify the structure of the intracellular domain of Robo1, thereby altering its signaling profile. Consistent with such a model, we have observed that the FLRT3-Robo1 interaction involves the cytoplasmic domain of Robo1 and that a large percentage of surface FLRT3 already colocalizes with Robo1 in rostral thalamic growth cones under basal conditions.

Our results showed that the Netrin-1 responsiveness involved in the topography of TCAs is determined by the expression and function of Robo1 and FLRT3. In the absence of FLRT3, such as in the case of wild-type iTCAs or rTCAs from *Flrt3* mutant mice, axons are not attracted to Netrin-1 in the corridor, so they target intermediate cortical regions. This ability depends on the presence of Robo1 receptor in these axons because the phenotype we found in *Robo1*$^{-/-}$ mimics the one found in *Flrt3* mutants. Furthermore, the absence of either Slit1 or Netrin-1 ligands in the vTel causes a similar caudal shift of rostral thalamocortical projections in vivo [21, 41, 42].

In summary, FLRT3 appears to modulate several developmental processes such as cell growth, cell migration, and axon guidance by interacting in *cis* or in *trans* with distinct transmembrane receptors. In TCAs, FLRT3 modulates the degree of responsiveness to Netrin-1 from a neutral response to attraction. Thus, our study shows a novel mechanism that allows switches in axon responses as development proceeds, such that there is no need to have a prior set of specific axon-guidance receptors. Instead, by simply introducing FLRT3 into the equation, the response to a given cue can be changed in function of the environment.

Experimental Procedures

Mouse Strains

Wild-type mice maintained on a CD1 background were used for gene-expression analysis and for tissue culture experiments. *Robo1* and *Robo1;Robo2* double-mutant heterozygous mice [43–45] were maintained on a CD1 genetic background and crossed to produce homozygous embryos. *Robo2* heterozygous mice [43–45] were maintained on a C57Bl/6 genetic background and crossed to produce homozygous embryos. *Dcc* heterozygous mice [46] were maintained on a 129SV/SvPasCrl genetic background and crossed to produce homozygous embryos. The *FLRT3*$^{\beta gal}$ allele is a reporter/null allele in which the coding sequence of the *FLRT3* gene was replaced by the gene β-galactosidase [47]. The *FLRT3*^{lx} allele carries two loxP sites flanking the third exon, which includes the entire coding sequence of the *FLRT3* gene. This allele was successfully validated and published previously [15]. In the present study, *FLRT3*$^{lx/lx}$ mice were crossed with the nervous-system-specific *Nestin*^{Cre} line [48], heterozygous for *FLRT3* (*FLRT3*$^{\beta gal/+}$), in order to obtain knockout brains from *FLRT3*$^{\beta gal/lx}$;*Nestin*$^{Cre/+}$ embryos. *FLRT3*$^{lx/lx}$ mice were also crossed with the inducible thalamic-specific *Gbx2*^{CreER} line [49], heterozygous for *FLRT3* (*FLRT3*$^{lx/+}$), in order to obtain brains from *FLRT3*$^{lx/lx}$;*Gbx2*$^{CreER/+}$ embryos with the specific FLRT3 deletion from the thalamus. The *Gbx2*^{CreER} line was provided by James Li (University of Connecticut Health Center). This line expresses *CreER(T2)-ires-EGfp* under the control of the *Gbx2* promoter. Tamoxifen induction of Cre recombination in *FLRT3*$^{lx/lx}$;*Gbx2*$^{CreER/+}$ embryos was performed by gavage administration of 5 mg tamoxifen (Sigma) dissolved in corn oil (Sigma) at E10.5 and E13.5 to maximize recombination in rostral thalamic structures [49, 50] (H. Gezelius, N. Anton-Bolaños, and G.L.-B., unpublished data). In all cases, the day of vaginal plug was considered to

(J and K) *Flrt3*-electroporated iTCAs from *Robo1*$^{+/+}$ embryos grow rostrally (J), whereas *Flrt3*-electroporated iTCAs grow at rostro-intermediate positions into the ventral telencephalon in the absence of *Robo1* (K).

(L) Quantification of the data represented in (J) and (K). n = 8 full-length *Flrt3* electroporated cocultures from *Robo1*$^{+/+}$; n = 6 full-length *Flrt3* electroporated cocultures from *Robo1*$^{-/-}$. ***p < 0.001 between distributions; *p < 0.05, **p < 0.01 and ***p < 0.001 between particular points, two-way ANOVA test.

(M) Experimental paradigm used to test the PKA activity in FLRT3 overexpressing iTCAs.

(N–O′) Phospho-I-1 staining of control-electroporated (N) or *Flrt3*-electroporated (O) E13.5 intermediate thalamic growth cones cultured for 48 hr when stimulated with rSlit1 (0.25 μg/ml) plus rNetrin-1 (0.5 μg/ml) for 20 min. GFP expression is shown in green.

(P) Quantification of the data represented in (N) and (O) and data not shown. n ≥ 63 growth cones per condition. *p < 0.05, two-tailed Student's t test.

iTh, intermediate thalamus; rSlit1, recombinant Slit1 protein; ID, integrated density. The data are presented as mean + SEM. Scale bars represent 150 μm (B and C), 300 μm (F and G; J and K), and 5 μm (N–O′). See also Figure S6.

Please cite this article in press as: Leyva-Díaz et al., FLRT3 Is a Robo1-Interacting Protein that Determines Netrin-1 Attraction in Developing Axons, Current Biology (2014), http://dx.doi.org/10.1016/j.cub.2014.01.042

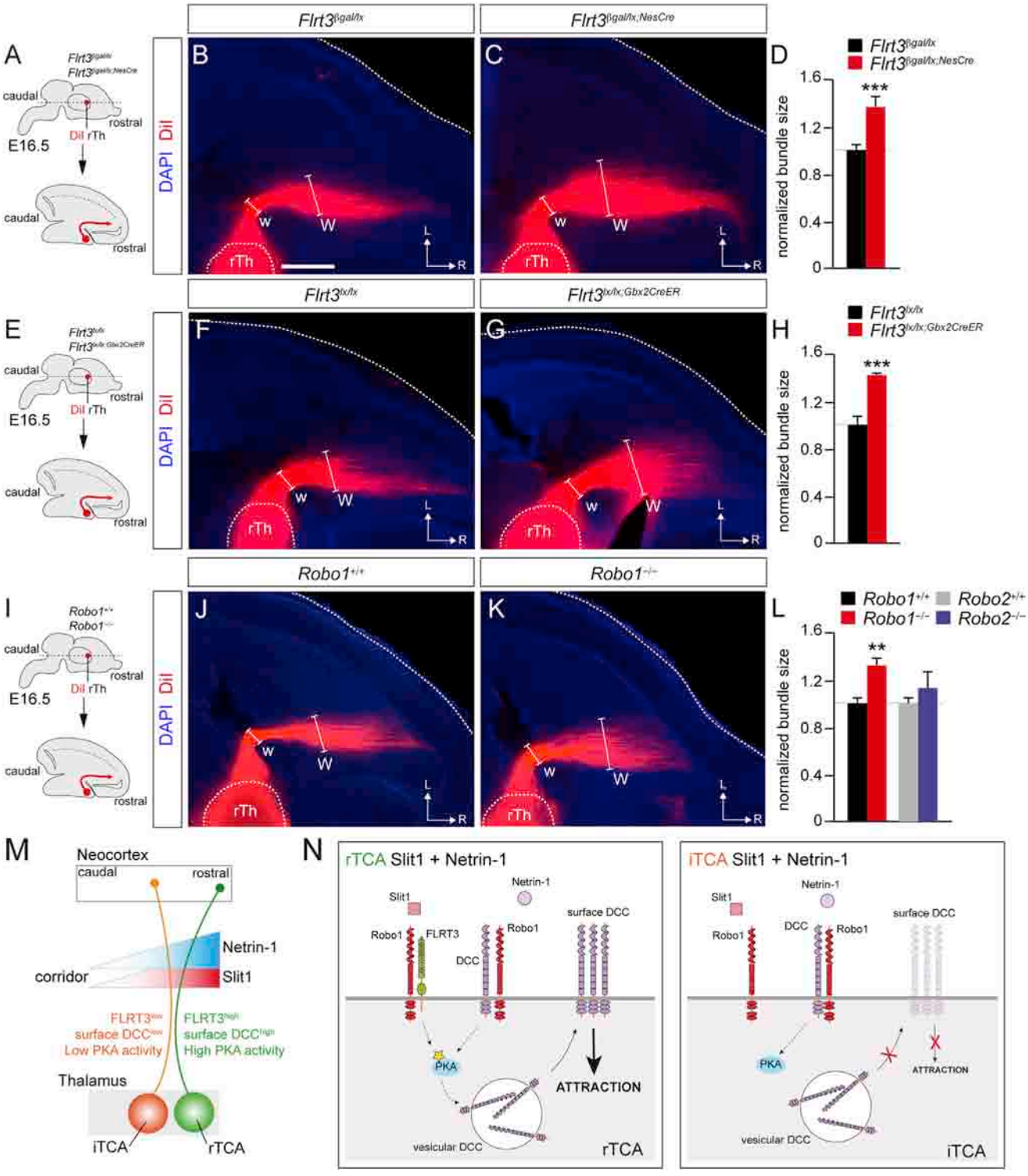

Figure 7. Abnormal Pathfinding of TCAs in the Absence of FLRT3 In Vivo

(A) Experimental paradigm used to trace rTCAs in *Flrt3*$^{\beta gal/lx}$ and *Flrt3*$^{\beta gal/lx;NesCre}$ at E16.5 embryos.

(B and C) Control (*Flrt3*$^{\beta gal/lx}$) rTCAs grow rostrally as a compact bundle (B), whereas they disperse to more intermediate regions of the vTel in *Flrt3*$^{\beta gal/lx;NesCre}$ brains (C), as revealed by the width of the bundle within the subpallium ("W") relative to its width at its entrance ("w").

(D) Quantification of the data represented in (B) and (C). n = 10 *Flrt3*$^{\beta gal/lx}$ brains; n = 9 *Flrt3*$^{\beta gal/lx;NesCre}$ brains. ***p < 0.001, two-tailed Student's t test.

(E) Experimental paradigm used to trace rTCAs in *Flrt3*$^{lx/lx}$ and *Flrt3*$^{lx/lx;Gbx2CreER}$ at E16.5 embryos.

(F and G) *Flrt3*$^{lx/lx}$ rTCAs grow rostrally as a compact bundle (F), whereas they disperse to more intermediate regions of the vTel in *Flrt3*$^{lx/lx;Gbx2CreER}$ brains (G).

(H) Quantification of the data represented in (F) and (G). n = 6 *Flrt3*$^{lx/lx}$ brains; n = 6 *Flrt3*$^{lx/lx;Gbx2CreER}$ brains. ***p < 0.001, two-tailed Student's t test.

(I) Experimental paradigm used to trace rTCAs in *Robo1*$^{+/+}$ and *Robo1*$^{-/-}$ at E16.5 embryos.

(legend continued on next page)

Please cite this article in press as: Leyva-Díaz et al., FLRT3 Is a Robo1-Interacting Protein that Determines Netrin-1 Attraction in Developing Axons, Current Biology (2014), http://dx.doi.org/10.1016/j.cub.2014.01.042

be E0.5. All animal procedures were approved by the Committee on Animal Research at the University Miguel Hernández, and they were carried out according to Spanish, German, and European Union regulations.

In Situ Hybridization, Immunohistochemistry, Enzymatic Staining, and Axonal Tracing

For in situ hybridization, the animals' brains were fixed overnight in 4% paraformaldehyde (PFA) in PBS, and brain vibratome sections were collected (80 μm thick, Leica Microsystems). In situ hybridization for *Flrt3* [47], *Slit1*, and *Netrin-1* [21] was performed using standard protocols [15].

For immunostaining, cultured cells and explants or slices were fixed in 4% PFA for 10 or 30 min, respectively. Immunostaining was performed on the following: dissociated thalamic neurons, thalamic explants in matrigel or collagen pads, and cultured slices. The following antibodies were used: mouse anti-βIII Tubulin 1/1,000 (Covance); goat anti-DCC 1/100, goat anti-FLRT3 1/100, goat anti-Robo2 1/50, goat anti-Unc5C 1/100 (R&D Systems); rabbit polyclonal antiserum against Robo1 1/1,000 (kindly provided by Fujio Murakami, Osaka University); rabbit anti-GFP 1/1,000 (Molecular Probes); chicken anti-GFP 1/3,000 (Aves Labs); rabbit anti-Robo1 1/100 (Novus Biologicals); rabbit anti-phospho-I-1 1/500 (Novus Biologicals); rabbit anti-Vamp2 1/200 (Millipore) and rabbit anti-Rab11 1/200 (Invitrogen). For surface DCC staining, anti-DCC antibody (R&D Systems) staining was carried out at 4°C for 20 min in a humidified chamber prior to fixation in 4% PFA at 4°C for 20 min. The absence of anti-βIII Tubulin staining was assessed in parallel to confirm that the cells were not inadvertently permeabilized at this step. Cultures were then permeabilized and F-actin was labeled with Phalloidin. The secondary antibodies used were as follows: Alexa Fluor 488-, 555-, and 647-conjugated goat or donkey anti-rabbit/mouse/goat (Molecular Probes 1:400). Alexa Fluor 488-, 568-Phalloidin (Molecular Probes), or Phalloidin-Atto 633 (Sigma) was applied together with the secondary antibodies.

To stain for β-galactosidase activity, E13.5 mouse brains were fixed for 1.5 hr in 0.2% glutaraldehyde and 1% PFA in PBS (containing 5 mM EGTA, 2 mM $MgCl_2$, and 0.02% NP40), and they were then immersed in 25% sucrose/PBS solution overnight at 4°C. Cryosections (14 μm) were stained for β-galacatosidase activity by incubating them for 2–3 hr at 37°C in a 1 mg/ml X-gal solution (Invitrogen) containing 5 mM $K_4Fe(CN)_6$ and 5 mM $K_3Fe(CN)_6$. After rinsing, the samples were counterstained with FastRed (Vector Laboratories). For axonal tracing, the brains of embryos were fixed overnight in 4% PFA, and then small DiI crystals (1,1′-dioctadecyl 3, 3, 3′, 3′-tetramethylindocarbocyanine perchlorate; Molecular Probes) were inserted into the rostral part of the thalamus after we hemidissected the brain. For double-labeling studies, small DiA crystals (4-4-dihexadecyl aminostyryl N-methyl-pyridinium iodide; Molecular Probes) were inserted into the intermediate part of the thalamus together with the DiI crystals. After the dyes were allowed to diffuse at 37°C, vibratome (100 μm) brain sections were obtained and counterstained with DAPI (Sigma), a fluorescent nuclear dye.

Thalamic Explants in Collagen or Matrigel

COS7 cells were transfected (FuGene HD, Promega) with expression vectors encoding the following proteins: human Slit1 [51], Netrin-1 [52], Gfp, or dsRed [53]. Aggregates were prepared by diluting the transfected cells in Matrigel (BD Biosciences) as described previously [53]. Thalamic explants were confronted with COS7 cells and embedded in rat tail collagen (BD Bioscience), except when confrontation assays were performed after slice electroporation in which Matrigel was used (BD Bioscience). Then explants were cultured for up to 48 hr in Neurobasal medium supplemented with B-27, 25 mM glucose, 2 mM glutamine, and 100 U/ml pen-strep (Invitrogen). Recombinant Slit1 (5 nM; R&D Systems), FLRT3-ECD [15] (1 μg/ml), a mouse anti-DCC antibody (AF5 clone; Abcam), or control mouse IgG was added to the culture media as indicated. After fixation in 4% PFA, axons were labeled using the mouse anti-βIII Tubulin antibody (Covance).

Slice Cocultures and In Vitro Focal Electroporation

Organotypic slice cultures of the embryonic mouse telencephalon were prepared and maintained for 48 hr, as previously described [53]. Telencephalic-receiving slices were cut at an angle of 45° between the horizontal and sagittal planes, while thalamic explants were dissected out from coronal slices previously subjected to focal electroporation, performed as described elsewhere [53]. The following DNA plasmids were used for electroporation at a concentration of 1.2 μg/μl: *FLRT3-IRES-Gfp* and the empty vector. All the plasmids were coelectroporated with a plasmid encoding *Gfp* at 0.9 μg/μl and mixed with 1% fast green (Sigma). Cocultures were maintained for 48 hr in Slice Culture Medium (SCM: 69% Basal Medium Eagle, 25% Hank's balanced salt solution [HBSS], 5% Normal Horse Serum, 50 mM glucose, 2 mM glutamine, and 100 U/ml pen-strep), and the dispersion of thalamic axons along the rostro-caudal axis was quantified by plotting with ImageJ software.

Collapse Assays

Dissociated thalamic cultures from E13.5 thalamus were performed as described previously [54]. After 48 hr of culture, neurons were incubated with 1 μg/ml Slit1 or PBS (control) for 30 min at 37°C, fixed, and labeled with Alexa Fluor 488-Phalloidin (1/500, Invitrogen) to analyze growth cone morphologies. Collapsed growth cones were scored as shown previously [15].

Western Blot and Immunoprecipitation

Neuron cultures were lysed in lysis buffer (50 mM Tris-HCl [pH 7.4], 150 mM NaCl, 2 mM EDTA, and 1% Triton X-100) supplemented with protease and phosphatase inhibitor cocktails (Roche). Protein lysates were clarified by centrifugation at 1,000 × *g* for 10 min. For immunoprecipitations, 200–400 μg of total protein lysates were diluted to 400 μl with lysis buffer and precleared for 1 hr at 4°C on gentle rotation with 150 μl of a protein G Sepharose bead slurry (50%, Sigma). Precleared lysates were incubated overnight at 4°C with the appropriate primary antibody (1 μg goat anti-Robo1, 1 μg goat anti-FLRT3; R&D Systems) and then for 3 hr with 40 μl of the protein G Sepharose bead slurry (50%). The beads were washed three times with lysis buffer and resuspended in SDS loading buffer. The protein extracts or immunoprecipitates were resolved on 8%–12% SDS-PAGE and transferred to a nitrocellulose membrane (Protran, Whatman). The membranes were then blocked for 45 min at room temperature with 5% nonfat powdered milk in Tris-buffered saline Tween-20 (TBS-T: 50 mM Tris-HCl, 150 mM NaCl [pH 7.4], 0.05% Tween-20) and probed overnight at 4°C with the following primary antibodies: goat anti-Robo1 1/200, goat anti-Robo2 1/200, goat anti-Unc5C 1/200, goat anti-FLRT3 1/1,000, goat anti-DCC 1/500 (R&D Systems), rabbit anti-phospho-(Ser/Thr) PKA substrate 1/2,000 (Cell Signaling Technology), or mouse anti-βIII tubulin 1/20,000 (Covance). The membranes were then incubated with a horseradish peroxidase (HRP)-conjugated secondary antibody (Sigma), and antibody binding was visualized by chemiluminescence (Immobilon Western, Millipore) in a Luminescent Image Analyzer LAS-1,000 Plus (Fujifilm).

Surface Biotinylation

After 2 days in vitro, thalamic neurons were treated as indicated and incubated for 20 min at 37°C during the treatments. The cells were washed twice with ice-cold PBS containing $MgCl_2$ and $CaCl_2$ (PBS^+; Sigma), and the cells were then incubated with 0.5 mg/ml EZ-Link-Sulfo-NHS-SS-Biotin (Thermo Scientific) diluted in PBS^+ at 4°C for 30 min. Excess biotin was quenched by washing it off three times for 5 min each in PBS^+ with 50 mM NH_4Cl. Finally,

(J and K) $Robo1^{+/+}$ rTCAs grow rostrally as a compact bundle (J), whereas they disperse to more intermediate regions of the vTel in $Robo1^{-/-}$ brains (K). (L) Quantification of the data represented in (J) and (K). rTCA dispersion at the vTel is normal in $Robo2^{-/-}$ brains. n ≥ 6 brains per condition. **p < 0.01, two-tailed Student's t test.

(M) Scheme representing the topographic guidance of rTCAs and iTCAs in the ventral telencephalon. Corridor cells express overlapping gradients of Slit1 and Netrin-1 [21]. The rostral positioning of rTCAs relies on the specific expression and function of FLRT3 in these axons that, via PKA, increase surface DCC levels through the Slit1/Robo1 interaction, thereby enabling Netrin-1 attraction. The topographic arrangement of iTCAs depends on the repulsive activity of Slit1, and, thus, it is independent of FLRT3.

(N) Scheme representing the mechanism by which responsiveness to Netrin-1 is achieved in TCAs. Only the combination of Slit1 plus Netrin-1 can activate a downstream intracellular cascade in rTCAs that activates PKA, thereby producing an increase in surface DCC expression by activating vesicular transport, ultimately favoring Netrin-1 attraction. This mechanism requires Robo1 and FLRT3 receptor activation, and it is not triggered in iTCAs because they do not express FLRT3.

rTh, rostral thalamus. The data are presented as mean + SEM. Scale bar represents 300 μm. See also Figure S7.

the cells were washed twice with cold PBS^{+}, lysed in biotinylation lysis buffer (50 mM Tris-HCl [pH 7.4], 150 mM NaCl, 5 mM EDTA, 1.25% Triton X-100, 0.25% SDS, and 5 mg/ml iodoacetamide), and supplemented with protease inhibitor cocktail (Roche). Immunoprecipitations were performed with high-capacity NeutrAvidin resin (Thermo Scientific). Samples were examined in western blots as described.

Quantification of the Growth of Axons in Collagen or Matrigel Pads

Explants were subdivided into four sectors, and the guidance effect was quantified by calculating the P/D ratio for each explant, where P and D represent the length of the 40 longest axons (measured with ImageJ software) extending into the quadrants that are proximal and distal to the COS7 cell aggregate, respectively. Once the mean P/D ratio for each condition was determined, a guidance index was calculated for each condition as previously described [21]. Student's t test was used for the comparisons between conditions.

Supplemental Information

Supplemental Information includes Supplemental Experimental Procedures and seven figures and can be found with this article online at http://dx.doi.org/10.1016/j.cub.2014.01.042.

Acknowledgments

We thank Imma Montoliu, Cristina Merino, and Luis Rodriguez for their outstanding technical assistance. We are grateful to Oscar Marín for advice and critical reading of the manuscript. We are also grateful to members of the López-Bendito and E. Herrera laboratories for the stimulating discussions and comments. E.L.-D. is supported by a CONSOLIDER fellowship from the Consejo Superior de Investigaciones Científicas (CSIC). E.L.-D. held a short-term European Molecular Biology Organization (EMBO) mobility fellowship. D.d.T. was funded by an EMBO long-term fellowship. This work was supported by grants from the Deutsche Forschungsgemeinschaft (SFB870 to R.K.), the Spanish MICINN (BFU2010-18055 to J.E. and BFU2012-34298 to G.L.-B.), FP7-PEOPLE-2011-CIG (PCIG9-GA-2011-293980 to J.E.), the CONSOLIDER programme CSD2007-00023, and an ERC grant (ERC-2009-StG_20081210 to G.L.-B.). J.E. is a Ramón y Cajal investigator (RYC-2008-03342). G.L.-B. is an EMBO Young Investigator.

Received: December 16, 2013
Revised: January 10, 2014
Accepted: January 10, 2014
Published: February 20, 2014

References

1. O'Donnell, M., Chance, R.K., and Bashaw, G.J. (2009). Axon growth and guidance: receptor regulation and signal transduction. Annu. Rev. Neurosci. *32*, 383–412.
2. Bradford, D., Cole, S.J., and Cooper, H.M. (2009). Netrin-1: diversity in development. Int. J. Biochem. Cell Biol. *41*, 487–493.
3. Round, J., and Stein, E. (2007). Netrin signaling leading to directed growth cone steering. Curr. Opin. Neurobiol. *17*, 15–21.
4. Williams, M.E., Wu, S.C., McKenna, W.L., and Hinck, L. (2003). Surface expression of the netrin receptor UNC5H1 is regulated through a protein kinase C-interacting protein/protein kinase-dependent mechanism. J. Neurosci. *23*, 11279–11288.
5. Bartoe, J.L., McKenna, W.L., Quan, T.K., Stafford, B.K., Moore, J.A., Xia, J., Takamiya, K., Huganir, R.L., and Hinck, L. (2006). Protein interacting with C-kinase 1/protein kinase Calpha-mediated endocytosis converts netrin-1-mediated repulsion to attraction. J. Neurosci. *26*, 3192–3205.
6. Bouchard, J.F., Moore, S.W., Tritsch, N.X., Roux, P.P., Shekarabi, M., Barker, P.A., and Kennedy, T.E. (2004). Protein kinase A activation promotes plasma membrane insertion of DCC from an intracellular pool: A novel mechanism regulating commissural axon extension. J. Neurosci. *24*, 3040–3050.
7. Moore, S.W., and Kennedy, T.E. (2006). Protein kinase A regulates the sensitivity of spinal commissural axon turning to netrin-1 but does not switch between chemoattraction and chemorepulsion. J. Neurosci. *26*, 2419–2423.
8. Bonanomi, D., Chivatakarn, O., Bai, G., Abdesselem, H., Lettieri, K., Marquardt, T., Pierchala, B.A., and Pfaff, S.L. (2012). Ret is a multifunctional coreceptor that integrates diffusible- and contact-axon guidance signals. Cell *148*, 568–582.
9. Hao, J.C., Adler, C.E., Mebane, L., Gertler, F.B., Bargmann, C.I., and Tessier-Lavigne, M. (2010). The tripartite motif protein MADD-2 functions with the receptor UNC-40 (DCC) in Netrin-mediated axon attraction and branching. Dev. Cell *18*, 950–960.
10. Ly, A., Nikolaev, A., Suresh, G., Zheng, Y., Tessier-Lavigne, M., and Stein, E. (2008). DSCAM is a netrin receptor that collaborates with DCC in mediating turning responses to netrin-1. Cell *133*, 1241–1254.
11. Karaulanov, E., Böttcher, R.T., Stannek, P., Wu, W., Rau, M., Ogata, S., Cho, K.W., and Niehrs, C. (2009). Unc5B interacts with FLRT3 and Rnd1 to modulate cell adhesion in Xenopus embryos. PLoS ONE *4*, e5742.
12. Söllner, C., and Wright, G.J. (2009). A cell surface interaction network of neural leucine-rich repeat receptors. Genome Biol. *10*, R99.
13. O'Sullivan, M.L., de Wit, J., Savas, J.N., Comoletti, D., Otto-Hitt, S., Yates, J.R., 3rd, and Ghosh, A. (2012). FLRT proteins are endogenous latrophilin ligands and regulate excitatory synapse development. Neuron *73*, 903–910.
14. Böttcher, R.T., Pollet, N., Delius, H., and Niehrs, C. (2004). The transmembrane protein XFLRT3 forms a complex with FGF receptors and promotes FGF signalling. Nat. Cell Biol. *6*, 38–44.
15. Yamagishi, S., Hampel, F., Hata, K., Del Toro, D., Schwark, M., Kvachnina, E., Bastmeyer, M., Yamashita, T., Tarabykin, V., Klein, R., and Egea, J. (2011). FLRT2 and FLRT3 act as repulsive guidance cues for Unc5-positive neurons. EMBO J. *30*, 2920–2933.
16. Dudanova, I., and Klein, R. (2013). Integration of guidance cues: parallel signaling and crosstalk. Trends Neurosci. *36*, 295–304.
17. Fothergill, T., Donahoo, A.L., Douglass, A., Zalucki, O., Yuan, J., Shu, T., Goodhill, G.J., and Richards, L.J. (2013). Netrin-DCC signaling regulates corpus callosum formation through attraction of pioneering axons and by modulating Slit2-mediated repulsion. Cereb. Cortex. Published online January 17, 2013. http://dx.doi.org/10.1093/cercor/bhs395.
18. Stein, E., and Tessier-Lavigne, M. (2001). Hierarchical organization of guidance receptors: silencing of netrin attraction by slit through a Robo/DCC receptor complex. Science *291*, 1928–1938.
19. Evans, T.A., and Bashaw, G.J. (2010). Axon guidance at the midline: of mice and flies. Curr. Opin. Neurobiol. *20*, 79–85.
20. López-Bendito, G., and Molnár, Z. (2003). Thalamocortical development: how are we going to get there? Nat. Rev. Neurosci. *4*, 276–289.
21. Bielle, F., Marcos-Mondéjar, P., Leyva-Díaz, E., Lokmane, L., Mire, E., Mailhes, C., Keita, M., García, N., Tessier-Lavigne, M., Garel, S., and López-Bendito, G. (2011). Emergent growth cone responses to combinations of Slit1 and Netrin 1 in thalamocortical axon topography. Curr. Biol. *21*, 1748–1755.
22. Sann, S., Wang, Z., Brown, H., and Jin, Y. (2009). Roles of endosomal trafficking in neurite outgrowth and guidance. Trends Cell Biol. *19*, 317–324.
23. Han, J., Han, L., Tiwari, P., Wen, Z., and Zheng, J.Q. (2007). Spatial targeting of type II protein kinase A to filopodia mediates the regulation of growth cone guidance by cAMP. J. Cell Biol. *176*, 101–111.
24. Yam, P.T., Kent, C.B., Morin, S., Farmer, W.T., Alchini, R., Lepelletier, L., Colman, D.R., Tessier-Lavigne, M., Fournier, A.E., and Charron, F. (2012). 14-3-3 proteins regulate a cell-intrinsic switch from sonic hedgehog-mediated commissural axon attraction to repulsion after midline crossing. Neuron *76*, 735–749.
25. Keino-Masu, K., Masu, M., Hinck, L., Leonardo, E.D., Chan, S.S., Culotti, J.G., and Tessier-Lavigne, M. (1996). Deleted in Colorectal Cancer (DCC) encodes a netrin receptor. Cell *87*, 175–185.
26. Chédotal, A. (2007). Slits and their receptors. Adv. Exp. Med. Biol. *621*, 65–80.
27. Ypsilanti, A.R., Zagar, Y., and Chédotal, A. (2010). Moving away from the midline: new developments for Slit and Robo. Development *137*, 1939–1952.
28. Nishiyama, M., Hoshino, A., Tsai, L., Henley, J.R., Goshima, Y., Tessier-Lavigne, M., Poo, M.M., and Hong, K. (2003). Cyclic AMP/GMP-dependent modulation of Ca2+ channels sets the polarity of nerve growth-cone turning. Nature *423*, 990–995.
29. Shelly, M., Lim, B.K., Cancedda, L., Heilshorn, S.C., Gao, H., and Poo, M.M. (2010). Local and long-range reciprocal regulation of cAMP and cGMP in axon/dendrite formation. Science *327*, 547–552.
30. Tojima, T., Akiyama, H., Itofusa, R., Li, Y., Katayama, H., Miyawaki, A., and Kamiguchi, H. (2007). Attractive axon guidance involves asymmetric membrane transport and exocytosis in the growth cone. Nat. Neurosci. *10*, 58–66.

Please cite this article in press as: Leyva-Díaz et al., FLRT3 Is a Robo1-Interacting Protein that Determines Netrin-1 Attraction in Developing Axons, Current Biology (2014), http://dx.doi.org/10.1016/j.cub.2014.01.042

31. Moore, S.W., Correia, J.P., Lai Wing Sun, K., Pool, M., Fournier, A.E., and Kennedy, T.E. (2008). Rho inhibition recruits DCC to the neuronal plasma membrane and enhances axon chemoattraction to netrin 1. Development *135*, 2855–2864.
32. Hall, A., and Lalli, G. (2010). Rho and Ras GTPases in axon growth, guidance, and branching. Cold Spring Harb. Perspect. Biol. *2*, a001818.
33. Nguyen-Ba-Charvet, K.T., Brose, K., Marillat, V., Sotelo, C., Tessier-Lavigne, M., and Chédotal, A. (2001). Sensory axon response to substrate-bound Slit2 is modulated by laminin and cyclic GMP. Mol. Cell. Neurosci. *17*, 1048–1058.
34. Chalasani, S.H., Sabelko, K.A., Sunshine, M.J., Littman, D.R., and Raper, J.A. (2003). A chemokine, SDF-1, reduces the effectiveness of multiple axonal repellents and is required for normal axon pathfinding. J. Neurosci. *23*, 1360–1371.
35. Charoy, C., Nawabi, H., Reynaud, F., Derrington, E., Bozon, M., Wright, K., Falk, J., Helmbacher, F., Kindbeiter, K., and Castellani, V. (2012). gdnf activates midline repulsion by Semaphorin3B via NCAM during commissural axon guidance. Neuron *75*, 1051–1066.
36. Nawabi, H., Briançon-Marjollet, A., Clark, C., Sanyas, I., Takamatsu, H., Okuno, T., Kumanogoh, A., Bozon, M., Takeshima, K., Yoshida, Y., et al. (2010). A midline switch of receptor processing regulates commissural axon guidance in vertebrates. Genes Dev. *24*, 396–410.
37. Williams, S.E., Grumet, M., Colman, D.R., Henkemeyer, M., Mason, C.A., and Sakurai, T. (2006). A role for Nr-CAM in the patterning of binocular visual pathways. Neuron *50*, 535–547.
38. Kuwajima, T., Yoshida, Y., Takegahara, N., Petros, T.J., Kumanogoh, A., Jessell, T.M., Sakurai, T., and Mason, C. (2012). Optic chiasm presentation of Semaphorin6D in the context of Plexin-A1 and Nr-CAM promotes retinal axon midline crossing. Neuron *74*, 676–690.
39. Bellon, A., Luchino, J., Haigh, K., Rougon, G., Haigh, J., Chauvet, S., and Mann, F. (2010). VEGFR2 (KDR/Flk1) signaling mediates axon growth in response to semaphorin 3E in the developing brain. Neuron *66*, 205–219.
40. Falk, J., Bechara, A., Fiore, R., Nawabi, H., Zhou, H., Hoyo-Becerra, C., Bozon, M., Rougon, G., Grumet, M., Püschel, A.W., et al. (2005). Dual functional activity of semaphorin 3B is required for positioning the anterior commissure. Neuron *48*, 63–75.
41. Braisted, J.E., Catalano, S.M., Stimac, R., Kennedy, T.E., Tessier-Lavigne, M., Shatz, C.J., and O'Leary, D.D. (2000). Netrin-1 promotes thalamic axon growth and is required for proper development of the thalamocortical projection. J. Neurosci. *20*, 5792–5801.
42. Powell, A.W., Sassa, T., Wu, Y., Tessier-Lavigne, M., and Polleux, F. (2008). Topography of thalamic projections requires attractive and repulsive functions of Netrin-1 in the ventral telencephalon. PLoS Biol. *6*, e116.
43. Grieshammer, U., Le Ma, Plump, A.S., Wang, F., Tessier-Lavigne, M., and Martin, G.R. (2004). SLIT2-mediated ROBO2 signaling restricts kidney induction to a single site. Dev. Cell *6*, 709–717.
44. Long, H., Sabatier, C., Ma, L., Plump, A., Yuan, W., Ornitz, D.M., Tamada, A., Murakami, F., Goodman, C.S., and Tessier-Lavigne, M. (2004). Conserved roles for Slit and Robo proteins in midline commissural axon guidance. Neuron *42*, 213–223.
45. Ma, L., and Tessier-Lavigne, M. (2007). Dual branch-promoting and branch-repelling actions of Slit/Robo signaling on peripheral and central branches of developing sensory axons. J. Neurosci. *27*, 6843–6851.
46. Fazeli, A., Dickinson, S.L., Hermiston, M.L., Tighe, R.V., Steen, R.G., Small, C.G., Stoeckli, E.T., Keino-Masu, K., Masu, M., Rayburn, H., et al. (1997). Phenotype of mice lacking functional Deleted in colorectal cancer (Dcc) gene. Nature *386*, 796–804.
47. Egea, J., Erlacher, C., Montanez, E., Burtscher, I., Yamagishi, S., Hess, M., Hampel, F., Sanchez, R., Rodriguez-Manzaneque, M.T., Bösl, M.R., et al. (2008). Genetic ablation of FLRT3 reveals a novel morphogenetic function for the anterior visceral endoderm in suppressing mesoderm differentiation. Genes Dev. *22*, 3349–3362.
48. Tronche, F., Kellendonk, C., Kretz, O., Gass, P., Anlag, K., Orban, P.C., Bock, R., Klein, R., and Schütz, G. (1999). Disruption of the glucocorticoid receptor gene in the nervous system results in reduced anxiety. Nat. Genet. *23*, 99–103.
49. Chen, L., Guo, Q., and Li, J.Y. (2009). Transcription factor Gbx2 acts cell-nonautonomously to regulate the formation of lineage-restriction boundaries of the thalamus. Development *136*, 1317–1326.
50. Li, K., Zhang, J., and Li, J.Y. (2012). Gbx2 plays an essential but transient role in the formation of thalamic nuclei. PLoS ONE *7*, e47111.
51. Brose, K., Bland, K.S., Wang, K.H., Arnott, D., Henzel, W., Goodman, C.S., Tessier-Lavigne, M., and Kidd, T. (1999). Slit proteins bind Robo receptors and have an evolutionarily conserved role in repulsive axon guidance. Cell *96*, 795–806.
52. Serafini, T., Kennedy, T.E., Galko, M.J., Mirzayan, C., Jessell, T.M., and Tessier-Lavigne, M. (1994). The netrins define a family of axon outgrowth-promoting proteins homologous to C. elegans UNC-6. Cell *78*, 409–424.
53. López-Bendito, G., Cautinat, A., Sánchez, J.A., Bielle, F., Flames, N., Garratt, A.N., Talmage, D.A., Role, L.W., Charnay, P., Marín, O., and Garel, S. (2006). Tangential neuronal migration controls axon guidance: a role for neuregulin-1 in thalamocortical axon navigation. Cell *125*, 127–142.
54. Mire, E., Mezzera, C., Leyva-Díaz, E., Paternain, A.V., Squarzoni, P., Bluy, L., Castillo-Paterna, M., López, M.J., Peregrín, S., Tessier-Lavigne, M., et al. (2012). Spontaneous activity regulates Robo1 transcription to mediate a switch in thalamocortical axon growth. Nat. Neurosci. *15*, 1134–1143.